L-SHELL IONIZATION BY PROTONS OF 1.5 TO 4.25 MEV ENERGY

by

EUGENE MERLE BERNSTEIN

Date: April 6, 1954

Approved: Harold W. Lewis
Walter M. Nielsen
F. D. Stessel

A thesis

submitted in partial fulfillment
of the requirements for the
degree of Master of Arts
in the Graduate School
of Arts and Sciences
of
Duke University

1954

CONTENTS

	Introduction	vi
I	Experimental Procedure	1
II	Experimental Results	14
	Bibliography of Works Cited . . .	28

LIST OF FIGURES

Page

1. Detail of NaI Crystal Holder 3
2. Block Diagram of Electronics 3
3. Arrangement of Target and Scintillator . . . 5
4. Ta L-line, 2.5 Mev Proton Energy 11
5. Au L-line, 2.5 Mev Proton Energy 12
6. Pb L-line, 2.5 Mev Proton Energy 13
7. U L-line, 2.5 Mev Proton Energy 14
8. Angular Distribution of L X-rays from a Thin Au Target 17
9. Thick Target Yield vs. Proton Energy . . . 22
10. Cross-Sections for Production of L x-rays vs. Proton Energy 26

LIST OF TABLES

1. Relative Intensities for Ta, Au, Pb, and U L-series 7
2. Thick Target Yields 19
3. L x-ray Production and Ionization Cross-Sections 24

ACKNOWLEDGEMENTS

I wish to express my appreciation to Dr. H. W. Lewis for his suggestion of this project, and for his guidance and assistance in the performance of the experiment and in the preparation of this thesis.

I also wish to thank Dr. E. Merzbacher for many helpful discussions of the theory.

This work was supported by the United States Atomic Energy Commission.

E. M. B.

L - SHELL IONIZATION BY PROTONS OF 1.5 TO 4.25 MEV ENERGY

INTRODUCTION

Since heavy charged particles (protons, deuterons, and alpha particles) stopping in matter lose their energy by ionization and excitation processes, characteristic x-rays of the absorber are emitted. Measurement of the cross section for x-ray production, and application of corrections for the Auger effect, allow the cross-section for ionization to be obtained. In addition to the characteristic x-rays a small intensity of bremstrahlung is also produced and has been detected.(1)

Chadwick, in 1912, observed the characteristic x-rays emitted when alpha particles were stopped in matter.(2) Several other groups of workers have since studied the x-rays produced by alpha particles, deuterons, and protons.(3-12) The most recent investigation of x-rays produced by heavy particles was made at Duke University by Lewis, Simmons, and Merzbacher.(13,14) K-shell x-rays produced by protons of Van de Graaff energies on Mo, Ag, Ta, Au, and Pb were

studied. The measurements were made with a NaI scintillation counter. K-shell x-ray cross-sections were obtained as a function of proton energy and atomic number. These were converted to K-shell ionization cross-sections and compared with the non-relativistic theoretical ionization cross-sections calculated by Henneberg in 1933.(15) There was qualitative agreement between the experimental and theoretical values; however, significant quantitative discrepancies were noted.

The subject of this thesis is the measurement of L-shell x-ray production and ionization cross-sections produced by protons of 1.5 to 4.25 Mev energy. The techniques used are similar to those employed in the K-shell measurements described above; however, modifications in the experimental arrangement were necessary due to the fact the L x-rays are softer than K.

CHAPTER I

EXPERIMENTAL PROCEDURE

The L x-ray intensities were measured with a scintillation counter which consisted of a NaI (Tl) crystal mounted on a Dumont 6292 photomultiplier tube. Because of the low energy (< 15 kev) of the radiation to be detected, a thin window for the scintillator was essential to minimize absorption corrections. Also, the use of a scintillator about 2 mm. thick removed the background due to higher energy gamma and x-rays, but was still 100% efficient for the L x-rays.

Preparation of the NaI crystal, which is extremely hydroscopic, was made in the relatively moisture free atmosphere of a drybox. The crystal was reduced to the desired dimentions by grinding it in a mixture of 2 micron emory and alcohol against a glass plate. It was then cleaned by dipping in alcohol. The crystal was optically sealed to the bottom of its lucite housing (Figure 1) with white petroleum jelly. The

housing was coupled to the phototube in the same manner.[1] The phototube used was carefully selected from those available both for maximum signal to noise ratio and for maximum energy resolution.

Pulses produced in the phototube by single x-ray photons absorbed in the scintillator were fed through a cathode follower into a linear amplifier (standard Jordan-Bell) and then into a single channel pulse height analyzer (Atomic Instrument Co. Model 510). The window width was set at 1 volt according to the dial on the analyzer. Measurements made with a pulser showed that this setting corresponded to an actual window width of 0.8 volt. The amplifier was set on medium band. Maximum gain setting was used at all times since it was found that the best signal to noise level for a given phototube was obtained when the voltage on the tube was as low as possible. A Tektronix Model 511 A oscilloscope was used to monitor the output of the amplifier. A block diagram of the electronics is given in Figure 2.

The 47 kev Pb^{210} gamma-ray was used for energy calibration of the system. No extensive measurements were made since x-ray energies could be determined to within 10% with this single calibration point. This accuracy is sufficient for positive identification of L-series x-rays, and identification of these series is the only demand put upon the

---

[1] I wish to thank Mr. S. A. Cox for his helpful suggestions on cleaning the NaI crystal.

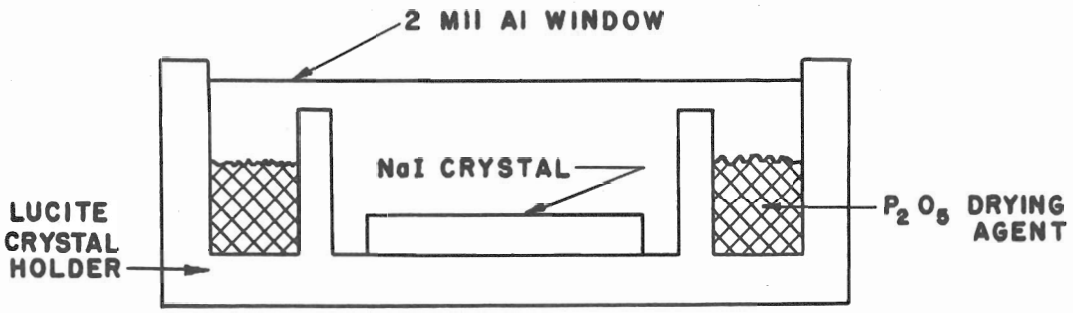

FIG. 1 - DETAIL OF NaI CRYSTAL HOLDER

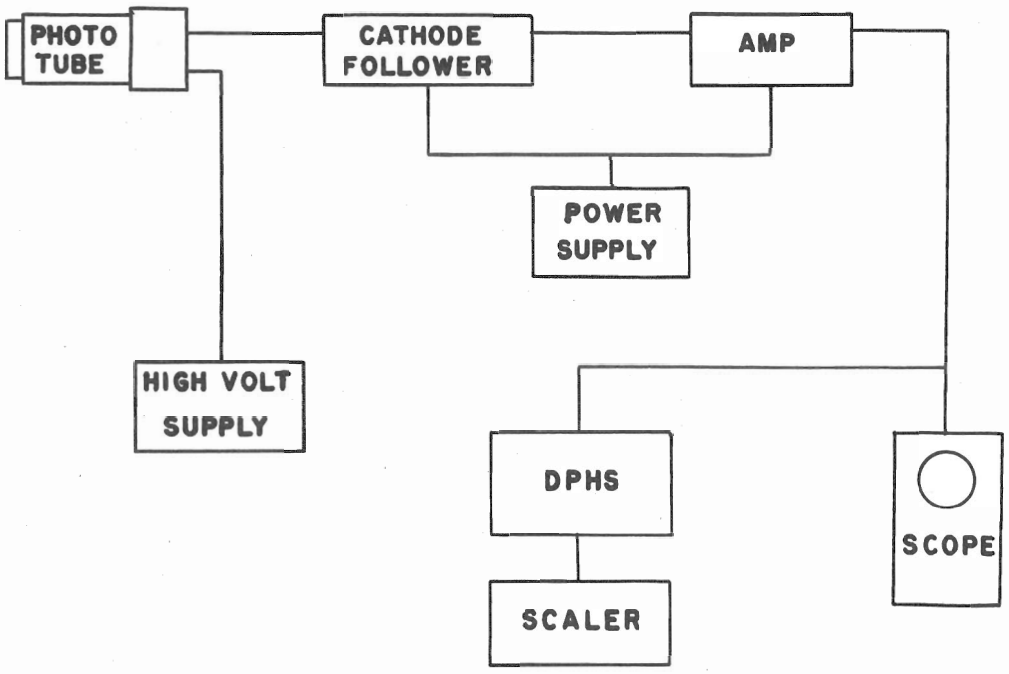

FIG. 2 - BLOCK DIAGRAM OF ELECTRONICS

system so far as energy determination is concerned.

The charge striking the target was measured with an electronic current integrator. (16) This integrator was calibrated artificially by a constant current source for a known time, yielding a calibration accuracy of better than 2%.

The proton accelerator used was, of course, the Duke University 4 Mev Van de Graaff machine. The proton energy was determined by the generating voltmeter which was previously calibrated by various known thresholds. The accuracy of the proton energy is estimated to be better than about 2%.

The targets were placed at an angle of 45° to the proton beam, so that with the scintillation counter set up at 90° to the beam the x-rays would have traveled the same distance from their point of production inside the target as the bombarding proton had traveled to that point. The mounting assembly consisted only of the target butting against an O-ring on the open end of the beam-tube, the thick target being held on by atmospheric pressure when the tube was evacuated. Again, to minimize absorption corrections, a piece of two mil mylar foil was used as an exit window on the target chamber. The arrangement of the target and scintillator is shown in Figure 3.

Due to the high intensities encountered it was necessary to back the scintillator off about four feet from the target. The x-rays were collimated by a lead diaphragm placed on top of the crystal. The portion of the crystal exposed to the x-radiation subtended a solid angle of 2.5×10^{-5} steradians.

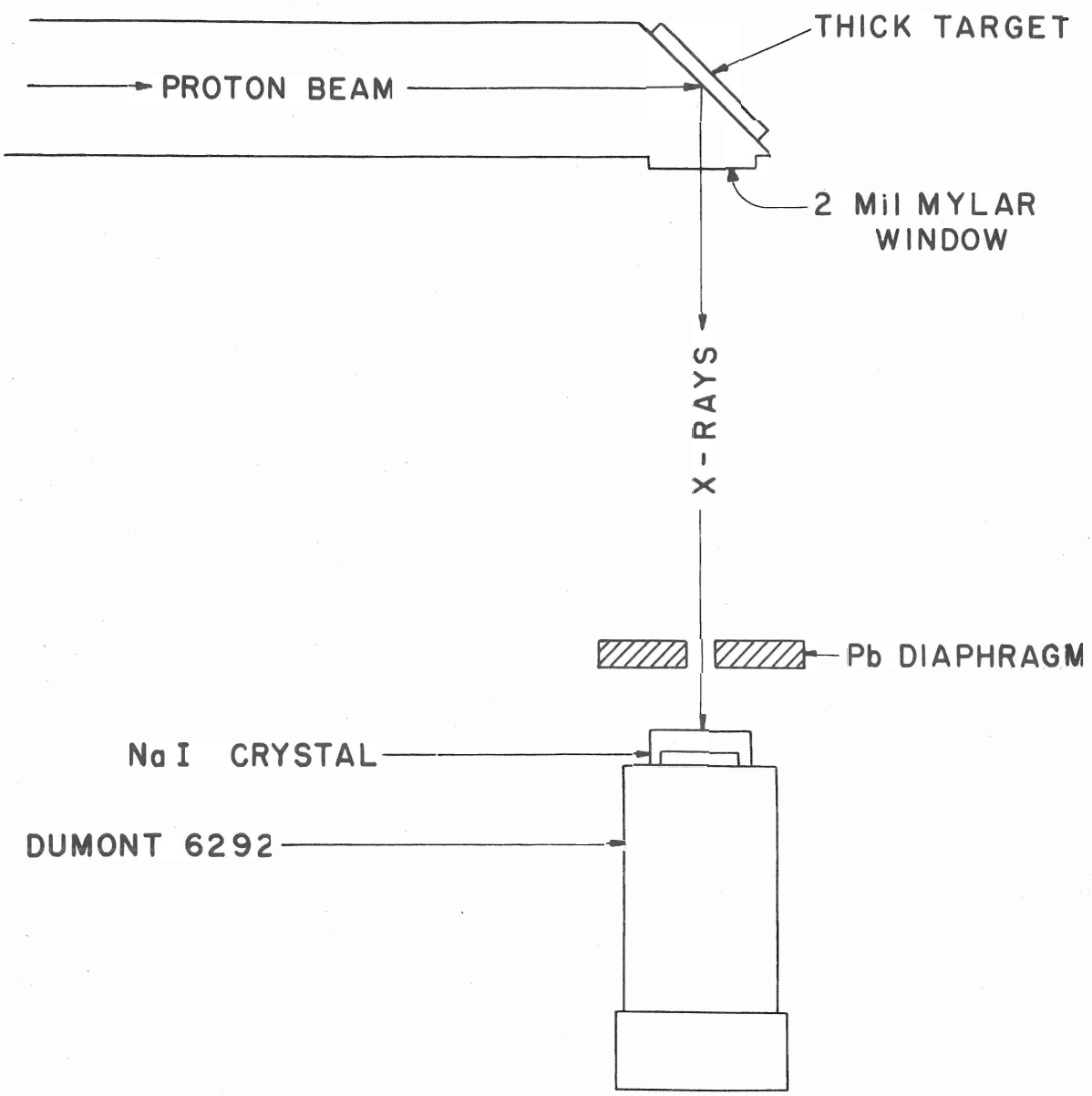

FIG. 3 - ARRANGMENT OF TARGET AND SCINTILLATOR

The targets used were selected to give as wide a spread in atomic number as possible. Since none of the rare earth elements (Z = 59 to Z = 72) were available for targets, the lowest Z element whose L x-rays were hard enough to be detected was Ta, Z = 73. Obviously the highest Z element was U. In addition to these two, the L x-rays from Au, Z = 79 and Pb, Z = 82 were investigated. In Table 1 are listed the wavelengths, energies, and relative intensities of the various lines in the L series for the four elements.(17) The weighted average wave-lengths and energies computed from the available intensities are given in section E of Table 1.

TABLE 1

Relative intensities for Ta, Au, Pb, and U L-series, $L_{\alpha 1}$ being taken as 100*

A. Ta L-series

	Line	Wave-length in Angstroms	Energy in kev	Relative Intensity
L_I	β_4	1.343	9.2	11
	β_3	1.304	9.47	16
	γ_3	1.103	11.16	8.5
	γ_2	1.097	11.2	5.9
L_{II}	β_1	1.324	9.3	103
	γ_1	1.135	10.9	31
L_{III}	α_2	1.530	8.06	10
	α_1	1.519	8.12	100
	β_2	1.282	9.6	40

B. Au L-series

L_I	β_4	1.104	11.2	5.2
	β_3	1.065	11.6	8.2
L_{II}	β_1	1.081	11.4	51
	γ_1	.925	13.3	11
L_{III}	α_2	1.285	9.6	11.4
	α_1	1.274	9.7	100
	β_2	1.068	11.5	23
		1.457	8.5	3.4

* Lines whose relative intensity are below 3 have been neglected.

TABLE 1 - Cont'd

C. Pb L-series

	Line	Wave-length in Angstroms	Energy in kev	Relative Intensity
L_I	β_4	1.00	12.3	5.2
	β_3	.967	12.8	8.2
L_{II}	β_1	.980	12.6	51
	γ_1	.838	14.7	11
L_{III}	α_2	1.184	10.4	11.4
	α_1	1.172	10.5	100
	β_2	.980	12.6	23
		1.347	9.16	3.4

D. U L-series

L_I	β_4	.746	16.5	4.1
	β_3	.709	17.4	4.2
L_{II}	β_1	.718	17.2	49
	γ_1	.613	20.1	12
L_{III}	α_2	.920	13.4	11
	α_1	.909	13.6	100
	β_2	.753	16.4	28
	β_5	.725	17.0	6.4

E. Weighted Average Wave-lengths and Energies for L-lines

Element	Z	Weighted Average Wave-length in Angstroms	Weighted Average Energy in kev
Ta	73	1.34	9.2
Au	79	1.17	10.6
Pb	82	1.07	11.6
U	92	.86	14.4

CHAPTER II

EXPERIMENTAL RESULTS

Figures 4,5,6, and 7 are some typical curves of counting rate against pulse height, normalized to 10μc. These have been corrected to give the number of counts in a one volt window. The width of the peaks is due partly to the presence of the several lines of the L-series which are not resolved, and partly to the finite resolution of the detection apparatus. Phototube noise overlaps slightly the low energy tail of the Ta, Au, and Pb curves. Pulse height curves such as these were taken at 250 kev intervals from 1.5 to 4.25 Mev.

The x-rays interact with the scintillator primarily by the photoelectric effect, thereby giving pulses corresponding to the full photon energy, provided the x-rays from iodine in the crystal are also absorbed. To calculate the number I of iodine x-rays which escape if I_o photons are incident on the crystal, one proceeds as follows. Since the beam of incident x-rays is collimated such that it strikes a small area in the

Fig. 4

Ta L - LINE
9.2 kev
Ep = 2.5 Mev

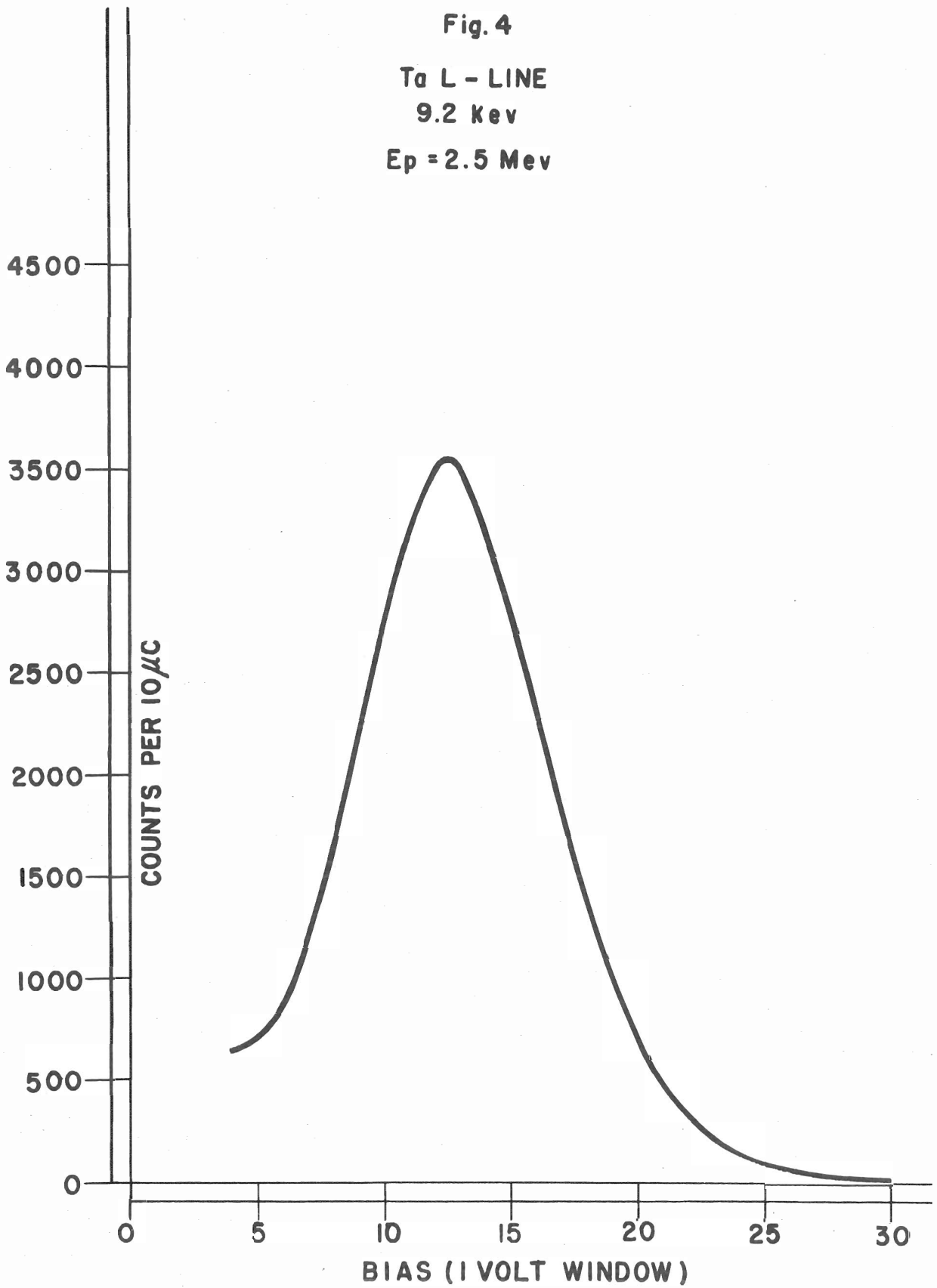

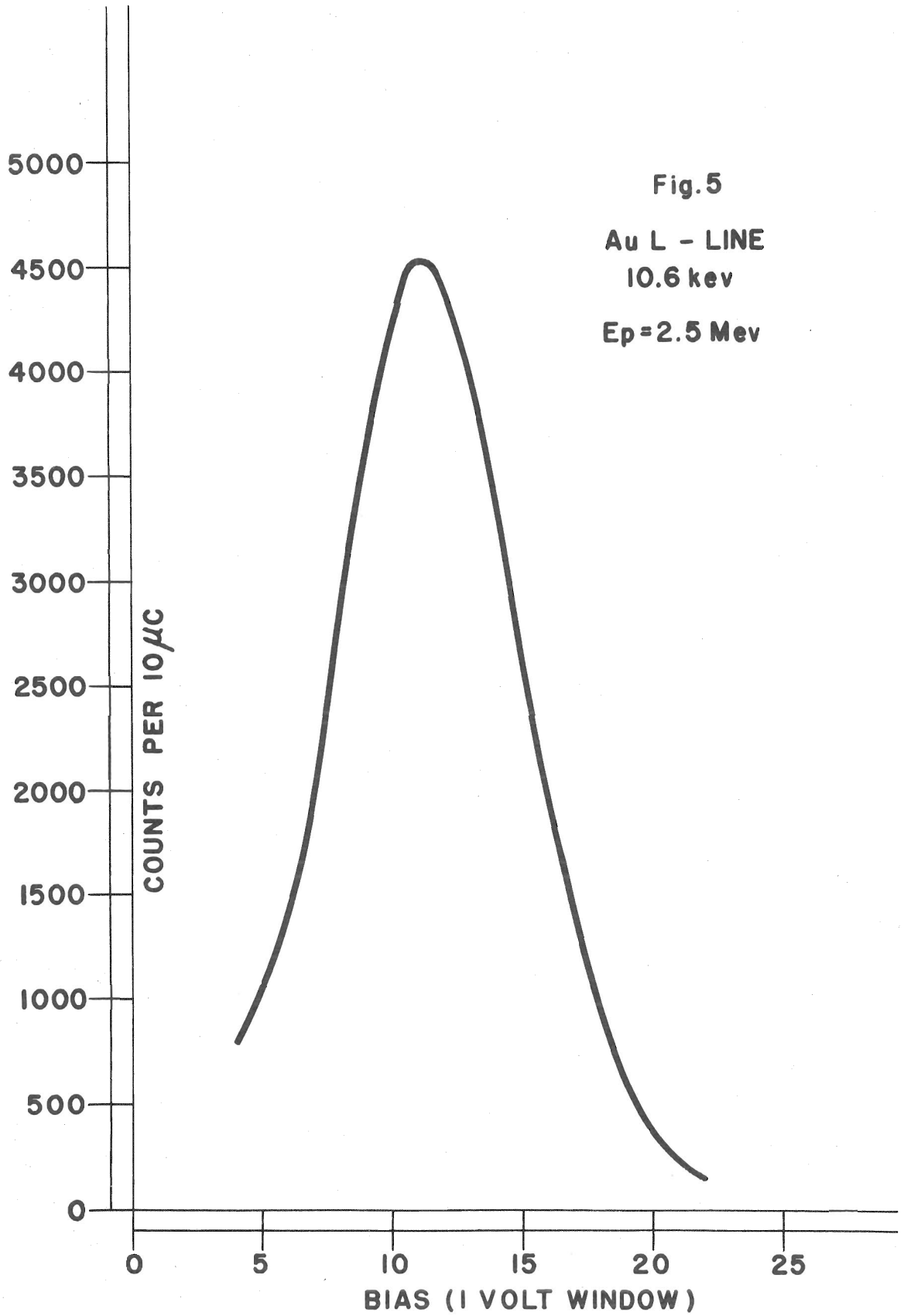
Fig. 5
Au L - LINE
10.6 kev
Ep = 2.5 Mev
5000
4500
4000
3500
3000
2500
2000
1500
1000
500
0
COUNTS PER 10 μC
0
5
10
15
20
25
BIAS (1 VOLT WINDOW)

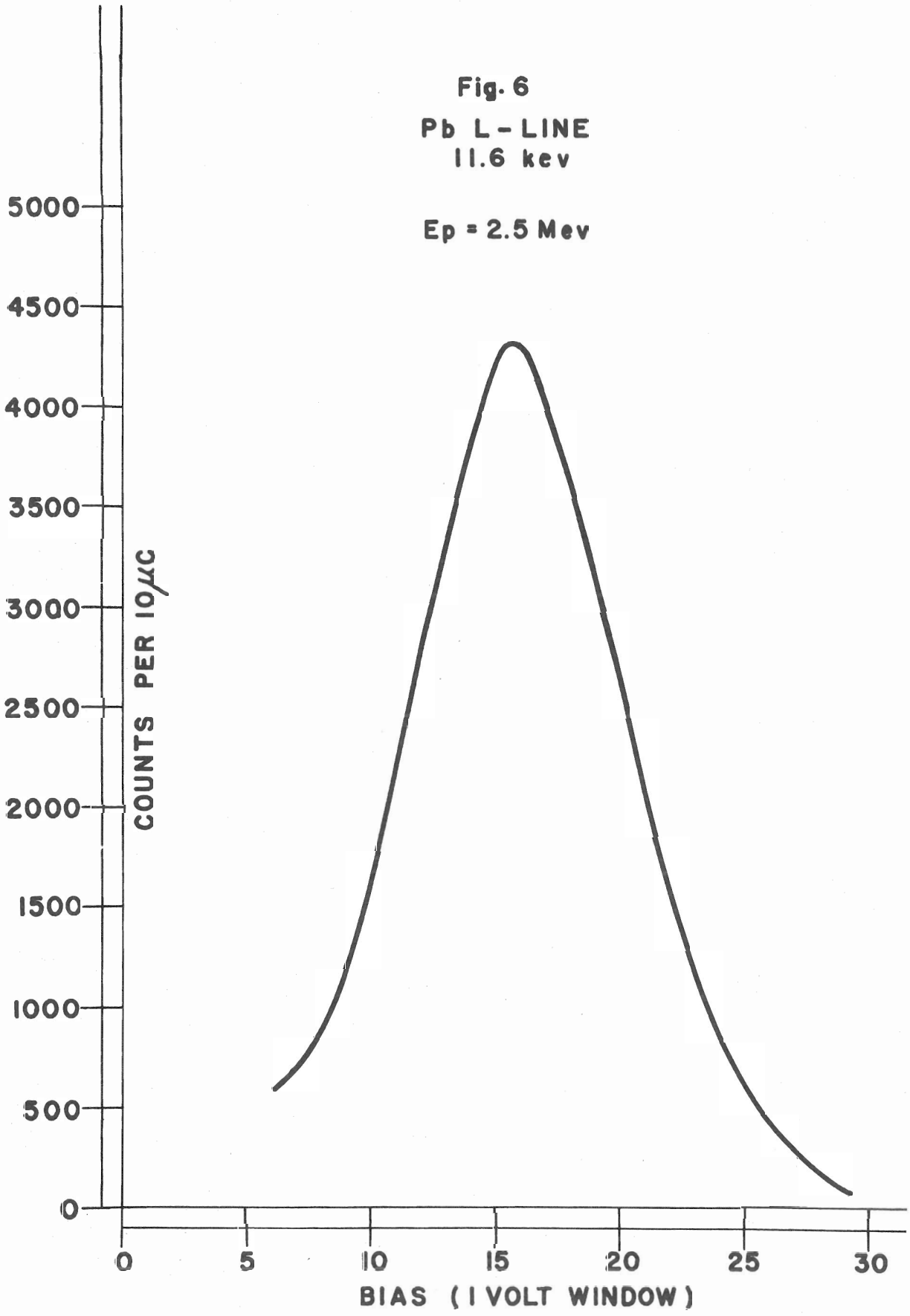
Fig. 6
Pb L - LINE
11.6 kev
Ep = 2.5 Mev
5000
4500
4000
3500
3000
2500
2000
1500
1000
500
0
COUNTS PER 10μC
0
5
10
15
20
25
30
BIAS (I VOLT WINDOW)

Fig. 7

U L - LINE
14.4 kev

Ep = 2.5 Mev

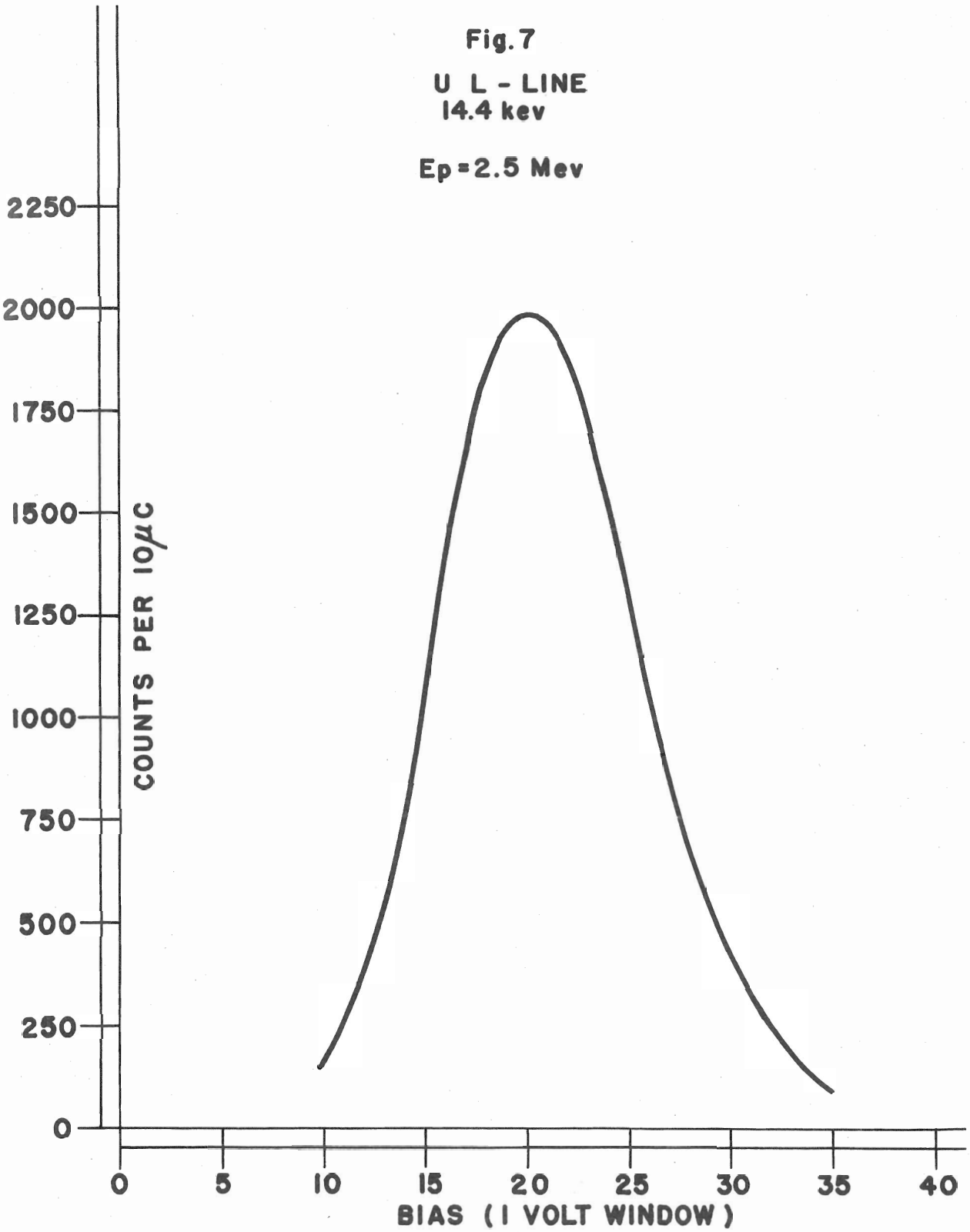

center of the crystal face, and since they penetrate only a small percentage of the depth of the crystal, the NaI crystal can be considered a semi-infinite medium. Then

$$I = \sum_j \alpha_j \beta_j \int_{X=0}^{\infty} \int I_o \mu_1 \, e^{-\mu_1 x} \, e^{-\mu_j x/\cos\theta} \, \frac{d\Omega}{4\pi} \, dx$$

The angle integration is over a solid angle of 2π and the summation is over all the electron shells in the iodine atom ($j = K,L,M,N,O$). α_j is the fraction of incident x-rays absorbed in the j^{th} shell. β_j is the ratio of j-shell x-ray emission to j-shell ionization (the other atoms undergo Auger transitions). X is the distance an incident photon penetrates the crystal before it is absorbed, θ is the angle between the direction of the incident photon and the escaping iodine x-ray. μ_1 is the absorption coefficient of NaI for the incident x-rays; μ_j is the absorption coefficient of the NaI for the x-rays from the j^{th} shell of iodine. Evaluation of the integral gives:

$$I = \sum_j \alpha_j \beta_j I_o \frac{1}{2}\left[1 - \mu_j/\mu_1 \ \ln(1 + \mu_1/\mu_j)\right]$$

Since the x-rays measured in this experiment are of lower energy than the iodine K absorption edge, $\alpha_K = 0$. Also, since the absorption of the incident photons in the iodine L-shell is much greater than the absorption in the remaining shells, it can be assumed that $\alpha_L = 1$ and $\alpha_M = \alpha_N = \alpha_O = 0$. This assumption leads to an escape intensity slightly greater than the actual case.

$\omega_L = .12$. Then

$$I = .06 I_0 \left[1 - \mu_L/\mu_1 \ \ln(1 + \mu_1/\mu_L) \right]$$

For Ta, which has the maximum escape of iodine x-rays of the elements investigated, $I = 1.5\% I_0$. Also, due to the finite resolution of the detection apparatus many of the degraded pulses caused by iodine x-ray escape are counted. Thus, even with the assumption made above any effect due to escape can be neglected.

An angular distribution of the L x-rays from a thin Au target was taken, and found to be isotropic to at least two percent. (Figure 8) Therefore, to obtains I_μ, the total yield of x-rays when one proton of initial energy E_p is stopped in the thick target, only the following calculations must be made:

(a) Find the integrated number of counts under the counting rate vs bias curve, and devide by the number of current integrator counts (1.03 μc) per integrator count). This gives the number J of photons counted per $N = 6.42 \times 10^{12}$ incident protons. The values of J are listed in column 5 of Table 2.

(b) Apply the correction for a solid angle $\Omega = 2.5 \times 10^{-5}$ steradians.

(c) Correct for the absorption of the x-radiation in the thin windows and air.

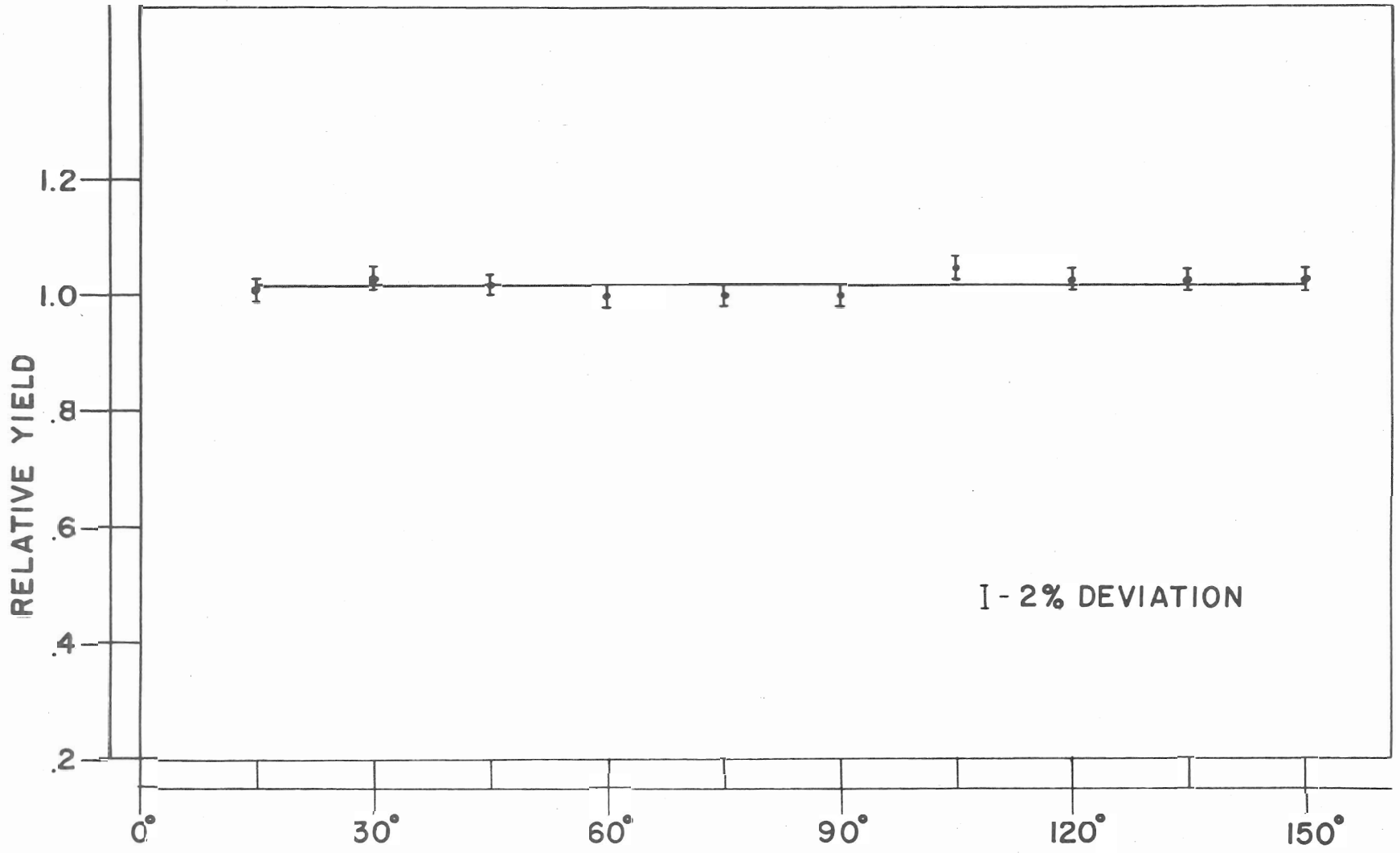

FIG. 8 - ANGULAR DISTRIBUTION OF L X-RAYS FROM A THIN Au TARGET - NORMALIZED AT 90°

The absorption corrections for the thin windows were determined experimentally by inserting additional window material, two mils of mylar foil and two mils of aluminum foil between the target and the scintillator. The air absorption correction was calculated, using the weighted average x-ray wavelengths given in Table 1 and known absorption coefficients. C, the overall absorption correction factors are given in column 6 of Table 2.

Then

$$I_\mu = \frac{4\pi CJ}{\Omega N} \qquad (1)$$

The calculated values of I_μ are given in column 7 of Table 2.

To calculate the cross-section for x-ray production one must take account of the self-absorption of the target for its own radiation, and the slowing down of the proton as it penetrates the thick target. Proceeding in the same manner as Reference 14, the number of x-ray quanta emitted from a thick target into a solid angle Ω per N incident protons of energy E and range x_o is given by

$$CJ = \frac{\Omega}{4\pi} Nn\rho \int_0^{x_o} e^{-u(x_o - x)} \sigma\left[E(x)\right] dx \qquad (2)$$

where $\sigma\left[E(x)\right]$ denotes the cross-section for ionization with x-ray emission. μ is the absorption coefficient of the target for its own x-rays, n denotes the number of target atoms per gram, and ρ is the density of the target.

TABLE 2

Yields of L-Shell X-Rays

1	2	3	4	5	6	7
Element	Z	E_L in kev	E_p in Mev	J	C	I_μ
Ta	73	9.2	1.50	0.77×10^3	4.55	3.0×10^{-4}
			1.75	1.3		5.1
			2.00	2.2		8.6
			2.50	3.8		1.5×10^{-3}
			3.00	5.8		2.26
			3.25	7.3		2.8
			3.50	8.2		3.2
			3.75	9.8		3.8
			4.00	11.1		4.3
			4.25	12.3		4.8
Au	79	10.6	1.50	0.71×10^3	2.60	1.6×10^{-4}
			1.75	1.35		3.0
			2.00	2.1		4.7
			2.25	3.2		7.2
			2.50	4.0		8.9
			2.75	5.2		1.17×10^{-3}
			3.00	6.9		1.53
			3.25	8.5		1.9
			3.50	9.6		2.2
			3.75	11.4		2.5
			4.00	13		2.9
			4.25	14		3.1

TABLE 2 - Cont'd

1	2	3	4	5	6	7
Element	Z	E_K in kev	E_n in Mev	J	C	I_μ
Pb	82	11.6	1.50	0.64×10^3	2.12	1.16×10^{-4}
			1.75	1.16		2.1
			2.00	1.9		3.5
			2.25	2.9		5.3
			2.50	4.1		7.5
			2.75	5.5		1.0×10^{-3}
			3.00	6.5		1.2
			3.25	8.7		1.6
			3.50	10		1.8
			3.75	11.8		2.1
			4.00	13.5		2.4
			4.25	15.7		2.8
U	92	14.4	1.50	3.2×10^2	1.56	4.5×10^{-5}
			1.75	6.2		8.3
			2.00	9.5		1.3×10^{-4}
			2.25	1.5		2.0
			2.75	3.1		4.2
			3.00	3.9		5.3
			3.25	5.0		6.8
			3.50	6.3		8.5
			3.75	7.9		1.07×10^{-3}
			4.00	9.5		1.3

Combining relations (1) and (2) gives

$$I_\mu(x_o) = n\rho \int_0^{x_o} e^{-\mu(x_o - x)} \sigma\left[E(x)\right] \, dx \qquad (3)$$

By differentiation of (3)

$$\sigma\left[E(x)\right] = \frac{1}{n\rho} \frac{dI_\mu(x)}{dx} + \frac{\mu}{n\rho} I_\mu(x) \qquad (4)$$

or

$$\sigma\left[E(x)\right] = \frac{1}{n} \frac{dI_\mu(x)}{dE} \frac{dE}{d(\rho x)} + \frac{\mu}{n\rho} I_\mu \qquad (5)$$

The last expression gives the cross-section for x-ray production as a function of known parameters and I_μ. $\frac{dI_\mu}{dE}$ was obtained from the slope of the curves given in Figure 9. $\frac{dE}{d(\rho x)}$ is the well known specific energy loss. The values of the mass-absorption coefficients, $\frac{\mu}{\rho}$, are rather important since at high proton energies the second term in Equation (5) predominates over the first. Again, using the weighted average wave-lengths, the absorption coefficients were obtained from relations given by Siegbahn. (17) The values thus obtained were checked experimentally for Ta and Au. The computed average mass absorption coefficients employed were:

FIG. 9

THICK TARGET YIELD, I_μ
VS
PROTON ENERGY

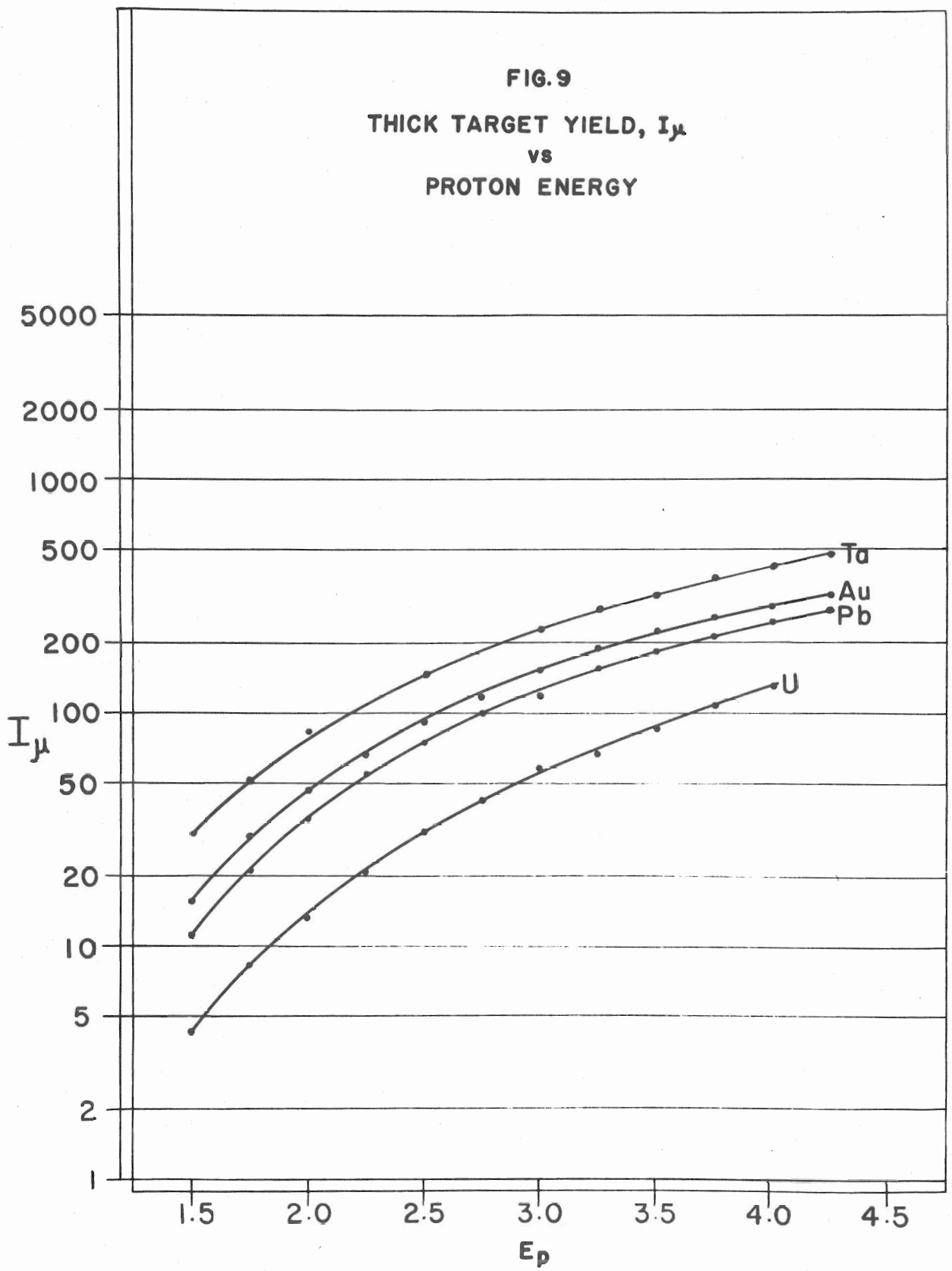

Element	Ta	Au	Pb	U
$(\mu/\rho)_{ave.}$ in cm^2/g	120	107	98	79

In column 3 of Table 3 are listed the cross-sections for L x-ray production, σ_{LX}. These are plotted as a function of proton energy in Figure 10. For Au the thick target results were supplemented by and found consistent with thin target measurements. An analysis of the errors involved in the determination of the absolute values of the x-ray production cross-sections indicate they are correct to 20% or better for all four elements.

As was mentioned previously, not all events in which an L electron is removed, result in L-shell x-ray emission. A radiationless (Auger) transition can occur, with the ejection of an electron from the excited atom. The total L-shell ionization cross-sections σ_{LI}, listed in column 5 of Table 3, are obtained by correcting σ_{LX} for Auger transitions. The Auger factors are not too well known, those used were the ones obtained by Lay in 1934 and given by Burhop. (18)

For comparison, Table 3 includes a few K-shell ionization cross-sections, σ_{KI}, taken from Reference 14. These are smaller than the L-shell cross-sections by several orders of magnitude. Although the L-shell cross-sections do not fit simple power laws in either proton energy or atomic number dependence, it was thought useful to determine the approximate variations

TABLE 3

L X-Ray and Ionization Cross-Section

1	2	3	4	5	6
Element	E_p in Mev	σ_{LX} in Barns	Auger Factor	σ_{LI} in Barns	σ_{KI} in Barns
Ta	1.50	24	3.56	84	
	1.75	36		126	
	2.00	54		192	0.017
	2.50	74		265	
	3.00	104		370	0.10
	3.25	124		440	
	3.50	139		495	0.20
	3.75	164		584	
	4.00	177		630	
	4.25	198		705	
Au	1.50	11.6	2.74	32	
	1.75	23		63	
	2.00	27		73	
	2.25	38		103	
	2.50	48		131	0.018
	2.75	59		161	
	3.00	74		203	
	3.25	85		233	
	3.50	96		263	
	3.75	105		288	
	4.00	116		318	
	4.25	126		345	

TABLE 3 - Cont'd

1	2	3	4	5	6
Element	E_p in Mev	σ_{LX} in Barns	Auger Factor	σ_{LI} in Barns	σ_{KI} in Barns
Pb	1.50	9.1	2.51	23	
	1.75	15		38	
	2.00	24		61	0.0045
	2.25	32		81	
	2.50	42		104	0.013
	2.75	48		122	
	3.00	54		134	0.032
	3.25	68		171	
	3.50	76		191	
	3.75	87		216	
	4.00	99		248	
	4.25	115		288	
U	1.50	3.4	2.22	7.6	
	1.75	6.2		14	
	2.00	9.0		20	
	2.25	13		28	
	2.50	16.5		37	
	2.75	20		45	
	3.00	24		54	
	3.25	30		67	
	3.50	38		83	
	3.75	46		103	
	4.00	56		123	

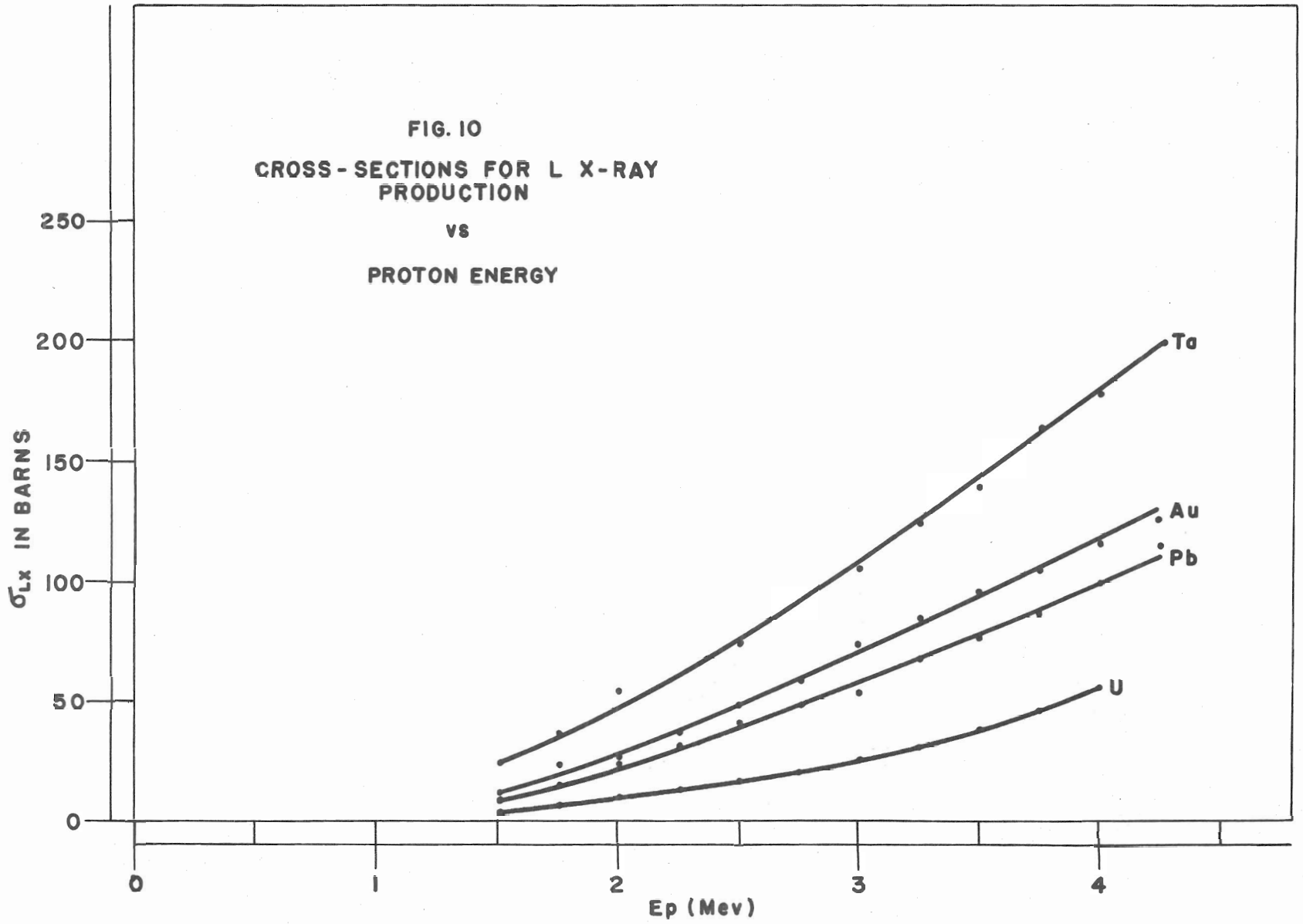
FIG. 10
CROSS-SECTIONS FOR L X-RAY PRODUCTION
vs
PROTON ENERGY
250
200
150
100
50
0
σ_{Lx} IN BARNS
Ta
Au
Pb
U
0
1
2
3
4
Ep (Mev)

for a comparison with the K-shell. The dependence on proton energy increases with increasing Z, being $E_p^{1.5}$ for Ta and E_p^2 for U. The atomic number dependence is $1/Z^8$. Thus, the L-shell variations are slower in both respects than the approximate E_p^4/Z^{12} variation of the K-shell.

BIBLIOGRAPHY OF WORKS CITED

1. C. Zupancic and T. Huus (private communication)
2. Chadwick, J. Phil. Mag. 24, 594 (1912)
3. Chadwick, J. Phil. Mag. 25, 193 (1913)
4. Chadwick, J., and A. S. Russel, Proc. Roy. Soc. 88, 217 (1913)
5. Chadwick, J., and A. S. Russel, Phil. Mag. 27, 112 (1914)
6. Rutherford, E. and H. Richardson, Phil. Mag. 25, 722 (1913)
7. Bothe, W. and H. Franz, Zeitschr. f. Physik, 52, 466 (1928)
8. Gerthsen, C. and W. Reusse, Phys. Zeitschr. 34, 478 (1933)
9. Barton, H. A., J. Franklin Inst. 209, 1 (1930)
10. Peter, Ann. d. Physik 27, 299 (1936)
11. Livingston, M. S., F. Genevese, and E. J. Konopinski, Phys. Rev., 51, 835 (1937)
12. Cork, J. M., Phys. Rev., 59, 957 (1941)
13. Simmons, B. E., The Production of Characteristic X-Rays by Proton Bombardment, Thesis, Duke University (1952)
14. Lewis, H. W., B. E. Simmons, and E. Merzbacher, Phys. Rev. 91, 943 (1953)
15. Henneberg, W., Zeitschr. f. Physik 86, 592 (1933)
16. Enge, H. A., Rev. Sci. Instr. 23, 599 (1952)
17. Seigbahn, M., Spektroskopie Die Roentgenstrahlen, Springer, Berlin (1931) p. 470
18. Burhop, E. H. S., The Auger Effect, University Press, Cambridge, (1952) p. 55